

We are IntechOpen, the world's leading publisher of Open Access books Built by scientists, for scientists

6,000

Open access books available

148,000

International authors and editors

185M

Downloads

Our authors are among the

154

Countries delivered to

TOP 1%

most cited scientists

12.2%

Contributors from top 500 universities



WEB OF SCIENCE™

Selection of our books indexed in the Book Citation Index
in Web of Science™ Core Collection (BKCI)

Interested in publishing with us?
Contact book.department@intechopen.com

Numbers displayed above are based on latest data collected.
For more information visit www.intechopen.com



Chapter

Applications and Data Analysis using Bayesian and Conventional Statistics in Biochar Adsorption Studies for Environmental Protection

*Obey Gotore, Tirivashe Phillip Masere, Osamu Nakagoe,
Vadzanayi Mushayi, Ramaraj Rameshprabu,
Yuwalee Unpaprom and Tomoaki Itayama*

Abstract

The use of low-cost agricultural waste-derived biochar in solving water and environmental challenges induced by climate change was investigated and sound conclusions were presented. Water reuse strategies can diminish the impact of climate change in rural and remote areas of developing countries. The novel biochar materials from three agro-waste biomass (Matamba fruit shell, Mushuma, and Mupane tree barks) were investigated and characterized to attest to their capacity to remove iodine from the aqueous solution. Their surface morphologies were assessed using Field Emission Scanning Electron Microscopy with Energy Dispersive X-Ray Spectroscopy (FESEM-EDX) which exhibited their structural phenomena to purge environmental pollutants. The Fourier-transform infrared spectroscopy (FTIR) was conducted to show surface functional groups of the biochar materials and Matamba fruit shell exhibited hydroxyl (-OH), carbonyl groups (C=O), C=C stretches of aromatic rings, and the carboxylate (C-O-O-) groups on its surface with corresponding data from the Isotherm and Kinetic models, statistically analyzed by the conventional and Bayesian methods. These surface mechanisms are said to be induced by weak van der Waals forces and π - π stacking interaction on the biochar surface. These adsorbents promised to be potential materials for environmental-ecosystem-protection and water re-use approach.

Keywords: adsorption, Bayesian statistics, Matamba fruit shell, Mushuma bark biochar, Mupane bark biochar

1. Introduction

Global warming and climate change is triggering some drastic global environmental complications and developing countries are facing cumulative water

insufficiency and such problems are subsequently increasing [1]. Some developing countries like Africa, South-East Asia, and South America are facing water deficits triggered by climate changes [2]. These countries are very vulnerable because of extremes of climatic change, which are increasing, their magnitude and frequency are making the availability of water a challenge to their societal livelihood's sustainability [3]. Portable safe water availability is becoming scarce due to high toxicity contaminants in water sources with a variety of constituents such as dyes [4] just to mention a few. Innovations, adaptations, and developments are being put in place to alleviate such burdens, and paramount measures are being employed to make sure that water is available and accessible to all in developing countries.

This study aims to remove micropollutants and recommend better wastewater reuse technology for unserved rural communities in an off-the-grid system to achieve socio-economic development using physicochemical properties of Mushuma, Mupani barks, and Matamba fruit shells, by analyzing their characteristics to evaluate the kinetic mechanism of adsorption from different models and statistical methods for the determination of equilibrium analysis. Thus, waste or residual biomass utilization such as biochar production has been given substantial attention because of its potential for carbon sequestration, waste management, and environmental remediation of pollutants [5]. A lot of technologies have been employed to mitigate challenges of water pollution globally, from a variety of sources and types of industries, for example, photocatalytic degradation [6], photooxidative degradation [7], Fenton reagent [8], and adsorption, wherein it is highly efficient in the removal of dyes and pigments from the liquid phase [9].

During the adsorption process, activated carbon is normally used due to its large specific surface area, well-developed pore structure, increased adsorption efficiency as well as good chemical stability [3]. [10] reiterated that adsorption takes place in the mesopores which act as conduits for adsorbate particles, and capillary condensation takes place to adsorb these macromolecules. The adsorption process has proved to be one of the best wastewater treatment technologies in the world and activated carbon acts as the universal adsorbent for the removal of different types of water pollutants. Most materials that come from carbon have great surface areas, which are stable with extensive functional groups, interconnected pore structures, and shapes [11]. To add to that, the Matamba fruit shell adsorption capacity, commonly found in Zimbabwe, can be a potential solution for water reuse techniques for the local people, and its kinetic adsorption was recently tested [11]. This can be attributed to adsorption as the most lucrative treatment technique [12], Langmuir and Freundlich's isotherms are common models which are extensively used since they are simple to use because of their empirical mathematical expressions [13].

The plant bark adsorbents for pollution reduction have widely been utilized in numerous studies which have been conducted recently [11]. Plant species analyzed included three eucalyptus, African border, flamboyant pods, and sycamore [14] among others. Biochar that is derived from waste biomass has also been considered one of the efficient adsorbents for wastewater pollutant removal because of its cost-effective merits, easy obtainability, and beneficial physicochemical properties [3]. The activated carbon materials, as adsorbents, has merits but are not limited to the adequate surface area, porosity phenomena, and thermal stability [15].

Different researchers are studying the application of biochar for wastewater treatment [5], and various materials are being pyrolyzed under different conditions and they can affect the physicochemical properties of the product [16]. The use of chemicals to modify the biochar by acids, bases, or polymers seems to give better

adsorption effectiveness because of enlarged surface area, modified chemical functionality, and availability of high-affinity adsorption sites [16]. Matamba, Mushuma, and Mupane tree barks as a novel and recent research for the removal of micropollutants as a wastewater re-use strategy or technology for unserved rural communities in an off-the-grid system to achieve socio-economic development.

2. Production of biochar

2.1 Biomass materials and pyrolysis conditions

Biochar is a material rich in carbon, produced from cracking several biomasses, such as wood, sludge, plants, food waste, and animal waste after carbonization [17, 18]. Such waste biomass materials exhibited to be effective for the removal of harmful substances from the aqueous solutions considering their less production cost and economic benefits, wide availability of raw material, and conducive surface properties. Furthermore, as noted by [5, 11, 19, 20], the use of biomass or residual waste has now been prioritized due to several advantages including environmental remediation, waste management, carbon sequestration, and ameliorating the greenhouse gas effect.

Pyrolysis is one of the most used technology in the production of biochar. It involves the carbonization of organic materials in limited or no oxygen conditions [21]. It is a thermochemical decomposition process taking place at temperatures above 300°C. In addition, the pyrolysis process may also produce volatile liquids and gases (e.g., carbon monoxide, carbon dioxide, hydrogen, methane, and biogas [22]). Pyrolysis may be categorized into four groups based on temperature conditions, reaction time, and heating rate. These are: slow, fast, flash, and intermediate, and of these slow and fast are the most common types [22]. In fast pyrolysis, the temperature and heating rates are higher than in slow pyrolysis. As such the process can be done in seconds and the resulting product consists mainly of bio-oils [23].

Conversely, in slow pyrolysis, the process can go on for hours and the heating rate and temperature are lower; a temperature under 450°C is commonly used and the resulting product is mainly biochar [22]. Biochar may be chemically modified using acids, bases, or polymers to have better adsorption efficiency due to the increased surface area, modified chemical functionality, and the presence of high-affinity adsorption sites [16]. The adsorption mechanism of the biochar after pyrolysis is shown on **Figure 1** where both positive and negative charges do exist on the surface due to thermal decomposition. This property enhancement process makes biochar a cost-effective choice hazardous material removal from the environment.

2.2 Availability of Matamba fruit shell

Matamba (monkey orange - *Strychnos* spp.) are widely distributed in Southern Africa and particularly in Zimbabwe, where they are generally found throughout the country, but more so in the Midlands Province [11, 24]. These fruits proliferate in semi-arid areas of Zimbabwe, with limited rainfall water, and produce the fruit in abundance [25, 26]. Depending on the season, excess production of the fruit varies and sometimes leads to its underutilization, and this can be seen in the highveld around Zimbabwe where fruit remains and disturbs the environment [24]. The *Strychnos* spp. fruit is extensively found in Zimbabwe, it is underutilized, and little or no consideration has been raised for potential commercialization due to limited

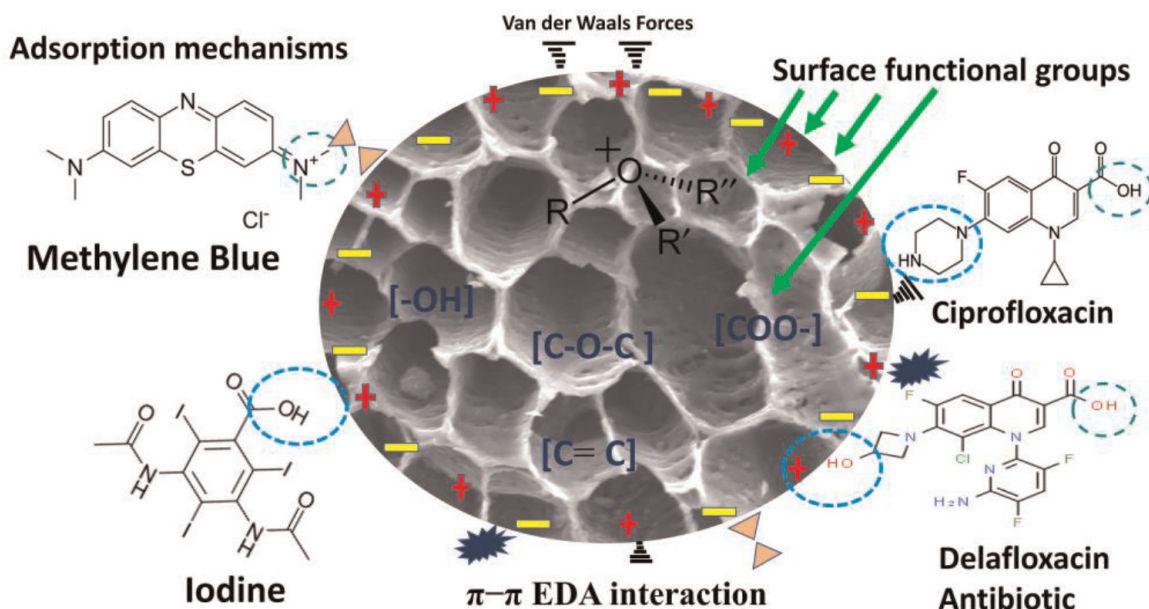


Figure 1.
The adsorption mechanism of adsorbates onto the biochar and surface characteristics after pyrolysis.

knowledge and dissemination of information about its propagation, agronomic practices, and product processing techniques for business [24].

The Matamba fruits begin to develop and grow during the autumn season and ripen in winter up to the spring season [11, 24]. The fruit is spherical with a hard thick shell, and the seeds are around 2–3 cm in diameter [11]. It is these seeds that are edible by humans and animals. To access these seeds the hard shells must be broken first, usually by hitting the shells on hard stone surfaces. After consumption of the seeds, the empty hard shells are often thrown away or littered around the veld or homesteads [24].

2.3 Agro-waste biomass

Agriculture and its related sectors like forestry generate massive volumes of biomass residues generated in the forestry in most developing countries. However, these residues should not be treated as waste given that a greater proportion of ‘waste’ is usable. As already discussed, pyrolysis is an important and more beneficial alternative to the usual farmer practice of burning, burying, or storing agricultural biomass residues [21, 27]. There is a large range of waste materials that could be suitable for pyrolysis and biochar production. However, for this study, agro-waste in the form of Mushuma, Mupane barks, and Matamba fruit shells were considered.

Mushuma tree, an African native species, is dominant in the Midlands province of Zimbabwe. The Shuma fruits (Jackle-berry, *Diospyros mespiliformis*) [28] are syrup-like juice and smooth with a soft-transparent-jelly inside. The tree has a medium to huge tree stem with the outer bark peeling off naturally as the tree grows as well as the season changes. The Mupane tree (*Colophospermum mopane*) [28] is a legume family vegetation abundantly found in the Midlands of Zimbabwe in hot, dry low-lying areas with an altitude ranging from 200 to 1150 meters above sea level.

The Mupane tree is also prevalent in South Africa, particularly in the Northwestern part of that country [29]. Tree barks of Mushuma and Mupane are usually used to start fires because of their common availability in the province as well as their affinity to fires. It is very quick to start fires and the tree wood itself takes a long time without

extinguishing. Generally, these trees' bark is either left in the forest after the tree ages or the outer barks peeled off or used as fuel by the local communities. However due to high rural to urban movements, the availability of tree barks is increasing, and the rest is getting decomposed in the bush with no value to the community.

3. Characterization of biomass materials

3.1 FESEM-EDX

In efforts to understand the thermal transformation and the structural setup of Mupane, Mushuma tree bark as well as the Matamba fruit shell biochar, it was necessary to characterize their surfaces with field emission scanning electron microscopy (FESEM) and energy-dispersive X-ray spectroscopy (EDX) after pyrolysis. These materials were characterized by using FESEM (JEOL JSM-7500FAM Tokyo, Japan) for surface morphology and image generation and EDX for element composition of biochar with a low vacuum. The pretreatment of the samples was conducted, where the biochar samples were dried at 105°C for 4 hours, stuck on the copper plate using a black double-sided tape, vacuumed for 12 hours, and analyzed for surface transformation.

The outcome of the EDX conducted revealed the purity of the elemental composition of Mushuma, Mupane barks, and the Matamba fruit shell biochar. Principally, the Matamba fruit shell biochar exhibited to be made up of 72.68 wt% C and some significant elements such as 10.35 wt%, 14.14 wt%, 0.97 wt%, 0.46 wt%, 0.37 wt%, and 0.31 wt% of O, N, K, Mg, Ca, P respectively with some trace compounds of Si and S as shown in **Table 1**.

It was revealed that adequate content of the C element remained after pyrolysis greatly influenced the adsorption capacity (44.071 mmol/g) of the biochar as ascribed by the Elovich kinetic model. Furthermore, the available O composition also offers enough polarization capability for high adsorption of the iodine used (43.65 mmol/g) as observed in the experimental data.

3.2 FTIR measurement

The Fourier transform infrared spectroscopy (FTIR) analysis was carried out using a wave number scanning range between 400 and 4000 cm^{-1} . Before that, the content of the moisture and ash that can be available in these materials was measured following the ASTM D1762–84 guide. The elemental compositional analysis of C, H, and N was executed accordingly. Acetanilide was used as a standard. Approximately 2 mg of biochar was used for each measurement, and each measurement was carried out in triplicate. The oxygen content (O) was then determined by the difference between the original dried sample and the sum of C, H, N, and ash content.

3.3 Surface area estimation using iodine solution

The results from the EDX and FESEM elemental presentation show a high content of Caborn with rigid skeleton structures of Matamba fruit shell, Mushuma, and Mupane bark which would be ascribed to the residual lignin from incomplete pyrolysis of the materials. Moreover, the weak van der Waals forces played a role in the removal of Iodine due to these high C, C/N, and O/C ratios which are inferred in **Table 2** and augmented biochar surface meso pore filling.

Material	Element	C*	N	O*	Na	Mg*	Al*	Si	P*	S*	Cl*	K*	Ca*	Mn*	Zn*
Mushuma biochar	ms%	74.76	nd*	19.6	nd*	0.45	0.03	nd*	0.11	0.03	0.06	0.23	4.51	0.07	0.15
	mol%	81.93	nd*	16.12	nd*	0.24	0.02	nd*	0.05	0.01	0.02	0.08	1.48	0.02	0.03
Mupane biochar	ms%	80.92	nd*	14.25	nd*	0.25	nd*	0.04	0.02	0.07	nd	0.07	4.18	0.04	0.16
	mol%	86.91	nd*	11.49	nd*	0.13	nd*	0.02	0.01	0.03	nd	0.02	1.34	0.01	0.03
Matamba biochar	ms%	72.68	14.14	10.35	nd*	0.46	0.04	0.02	0.31	0.22	0.02	0.97	0.37	nd*	nd*
	mol%	77.71	12.97	8.3	nd*	0.24	0.02	0.01	0.13	0.09	0.01	0.32	0.12	nd*	nd*

*nd not detected.

Table 1.
The elemental composition of Mushuma, Matamba, and Mupane biochar.

MODEL	Adsorbent	Model Parameter	Mean (\pm SD)	Bayesian statistical analysis					Conventional analysis			
				2.50%	25%	50%	75%	97.50%	Rhat	MAP	Mean	AICc
Langmuir	Matamba BC	KL (L /mol)	218.5 \pm 81.8	110.2	171.5	206.03	248.42	400.1	1.001	195.6	206.4 \pm 49.11	0.527
	Matamba BC	qmax (mmol/g)	2.12 \pm 0.12	1.886	2.05	2.118	2.188	2.363	1.001	2.11	2.12 \pm 0.089	
Freundlich	Matamba BC	KF (mmol L /mol)	3.061 \pm 0.40	2.3	2.8	3.1	3.3	3.892	1.001	3.08	3.08 \pm 0.295	5.377
	Matamba BC	mf [-]	0.194 \pm 0.04	0.11	0.2	0.2	0.2	0.282	1.027	0.2	0.196 \pm 0.032	
	Mushuma BC	k ₂ (g mmol/min)	0.014 \pm 0.002	0.011	0.013	0.014	0.016	0.019	1.002			
PSO	Mushuma BC	qt (mmol/g)	40.712 \pm 0.986	38.776	40.106	40.703	41.308	42.715	1.001			
	Mupane BC	k ₂ (g mmol/min)	0.014 \pm 0.002	0.011	0.013	0.014	0.015	0.019	1.002			
	Mupane BC	qt (mmol/g)	41.64 \pm 0.997	39.621	41.051	41.64	42.228	43.62	1.002			
	Mushuma BC	α (mmol/g/ min)	112.85 \pm 40.2	55.621	86.492	105.82	131.39	212.627	1.002			
Elovich	Mushuma BC	β (g/ mmol)	0.16 \pm 0.012	0.135	0.152	0.159	0.167	0.185	1.001			
	Mupane BC	α (mmol/g/ min)	120.2 \pm 52.72	53.172	84.764	108.84	142.87	256.495	1.001			
	Mupane BC	β (g/ mmol)	0.156 \pm 0.015	0.129	0.146	0.156	0.166	0.187	1.002			

Table 2. Shows both the Bayesian and conventional statistical analysis results for the biochar investigated using isotherm and kinetic models.

The remaining alkaline elements such as Ca, Mg, and K with inorganic basic minerals present might be ascribed to the main component of ash established from the pyrolysis process of the biochar [29, 30]. In summary, the Iodine adsorption mechanisms onto the investigated biochar materials made it a probable choice for environmental contamination option, water reuse possibility, and global warming reduction due to high C, C/N, and enough polarization propensity.

Regarding the biochar produced from Mushuma and Mupane barks, it was from the FESEM images above that surface texture can be influenced by biomass type even under identical pyrolysis conditions. Biochar produced from Mushuma bark has large surface pores (10–15 μm in diameter), uniformly distributed and separated by a thick carbon wall (2–3 μm) than Mupane bark. Biochar from Mupane bark had smaller and heterogeneously distributed pores (3–5 μm in diameter).

Similarly, the kinetic results from Iodine adsorption indicated that biochar from Mupane had higher q_t values than biochar from Mushuma bark. As found by [29], larger pores tend to correlate to the limited surface area than small pores, thus there is greater adsorption on smaller pores than on larger pores. Further, the small pores are associated with high porosity and void volume.

4. Equilibrium mechanisms of adsorbents and data analysis

4.1 Adsorption kinetics of Matamba fruit shell and the tree bark adsorbents

In principle, [31] elucidated that adsorption is known as the mass transfer method that entails some time for the adsorbate to diffuse from the bulk solution of the aqueous phase, through the solid–liquid film into the material's pore spaces and onto the available active sites. Therefore, based on the results obtained from the experiments kinetic models like pseudo-first-order (PFO), pseudo-second-order (PSO), intraparticle diffusion (IPD), and Elovich models are shown in **Table 3** and plotted as shown in **Figure 2a**.

MPNBC advocated more adsorption for Iodine than MSHBC as exhibited in **Figure 3c** and **d** correspondingly, however, Matamba fruit shell outperformed both tree barks. Subsequently, the Iodine kinetic adsorption mechanism on these materials could be divided into three stages: rapid adsorption stage, slow adsorption stage, and adsorption equilibrium stage as elucidated by [32] as well.

The first 12 hours were observed to be a rapid Iodine adsorption stage on both biochars. The graph for MPNBC seems to be steeper than MSHBC. The adsorption capacity of the prepared Mupane and Mushuma barks were estimated to be 40.38 and 39.78 mmol g^{-1} respectively, from the experimental data. From conventional statistical analysis of the Pseudo-second order model, Mushuma and Mupani biochar exhibited adsorption capacity of 40.01 and 40.29 mmol g^{-1} which were slightly lower than the Bayesian outcome of 40.712 and 41.639 mmol g^{-1} as shown in **Table 2**.

This reveals the strength of Bayesian analysis against classical statistics as different quantile ranges revealed different estimations and the 50% (median) was so close to the actual mean for each parameter. The adsorption rate constants of the two biochar also exhibited the above phenomenon where the conventional method indicated a homogeneous reaction rate (0.014 min^{-1}), so as the Bayesian statistics as shown in **Table 2**. The figures also elucidated that the linear relationship is presented not as a continuous straight line but in two stages of least and enormous adsorption before and after 4 hr. of adsorption respectively.

Kinetic model	Equations	Model parameter	Matamba	Mushuma	Mupane	Reference
PFO	$q_t = q_e(1 - \exp(-k_1t))$ (1)	qt (mmol/g)	40.08	37.28	38.2	Lagergren, 1898 (Eq. (1))
		k_1 (1/min)	0.232	0.4	0.41	
		AIC	59.05	51.52	51.14	
PSO	$q_t = \frac{q_e^2 k_2 t}{1 + q_e k_2 t}$ (2)	qt (mmol/g)	44.071	40.01	40.29	Ho and Makay, 1999 (Eq. (2))
		k_2 (g mmol/min)	0.0079	0.01	0.01	
		AIC	51.95	37.76	38.03	
IPD	$q_t = k_p t^{\frac{1}{2}} + C$ (3)	α (mmol/g/min)	45.41	110.7	117.88	Weber and Morris, 1963 (Eq. (3))
		β (g/mmol)	0.127	0.16	0.16	
		AIC	38.26	41.52	44.92	
		k_p (mmol/min)	7.72	3.64	3.66	
Elovich	$q_t = \left(\frac{1}{\beta}\right) \ln(\alpha\beta) + \left(\frac{1}{\beta}\right) \ln(t)$ (4)	C [-]	14.303	18.53	19.23	Bedin et al., 2016 (Eq. (4))
		AIC	46.56	54.29	55.94	

The AIC scores were used for non-linear model selection instead of the coefficient of determination (R^2).

Table 3. The kinetic adsorption equations and estimated parameters from biochar materials after the experiment.

The higher adsorption could be attributed to smaller biochar particle sizes (0.25–1.00 mm) used in this experiment which started to diffuse into the pores later since IPD is a slow process. The Elovich model revealed that the initial adsorption was 110.701 and 117.88 mmol g⁻¹ min⁻¹, 112.847 and 120.214 mmol g⁻¹ min⁻¹ for Mupane and Mushuma biochar from Conventional and Bayesian methods respectively.

Different adsorption mechanisms could have been encountered during the 48-hour contact time, but the adsorption rate gradually decreased until the adsorption reaches the equilibrium state as [28] elaborated. For Matamba biochar, Elovich (Eq. (3)) and IPD (Eq. (4)) better describe the kinetic adsorption of biochar through iodine adsorption than PFO (Eq. (1)) and PSO (Eq. (2)) models. Generally, the iodine adsorption rate decreases exponentially as the amount of iodine adsorbed increases on the heterogeneous surfaces of the Mushuma, Mushuma, and Matamba fruit shell biochar. Several adsorption experiments have been reported to follow the Elovich kinetic model [33, 34].

However, the adsorption kinetic results from conventional statistics on the tree bark revealed that the PSO kinetic model better described the adsorption behaviors of the biochar for Iodine adsorption [35, 36]. The model selection AICc scores for MPNBC and MSHBC were 38.03 and 37.76 respectively, away below other models used. AICc is a strong tool for model selection than using the correlation coefficient on non-linear model functions. This can be theoretically supported by the equilibrium adsorption capacity values from both statistical methods were also close to the experimental equilibrium adsorption capacity, signifying that the pseudo-second-order kinetic model could better describe the Iodine adsorption [36, 37]. From this point of

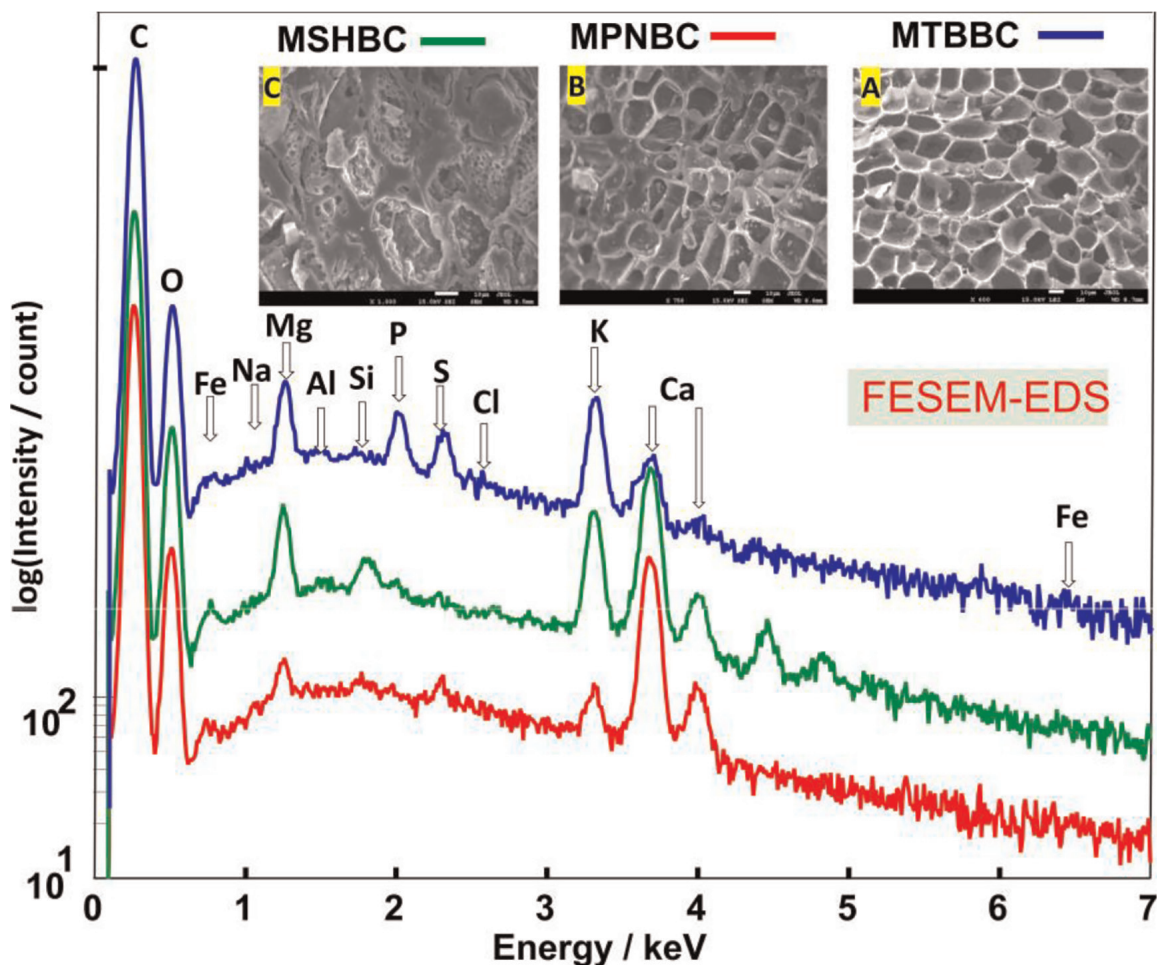


Figure 2. Elemental composition and FESEM analysis of (a) Matamba biochar (MTBBC), (b) Mupane tree bark (MPNBC), and (c) Mushuma tree bark (MSHBC).

view, it can be inferred that both conventional and Bayesian approaches to estimations are well established and seem hard to justify if one of the two is preferred over the other [38, 39]. It is thought that the π - π electron donor-acceptor (EDA) interaction is the main player with a major role in the iodine - adsorbent interaction since the adsorption capacity after 2 days of investigation. The strong interaction of π -donor and π -acceptor compounds full fills the EDA theory taking into consideration the FTIR results. As given in **Figure 4e**, the biochar materials also show various surface functional groups. Regarding **Figure 4e**, the peaks at 3334 cm^{-1} and $1764\text{--}1710\text{ cm}^{-1}$, can be ascribed to the hydroxyl groups (-OH) and the carbonyl groups (C=O) correspondingly. The shallow peak at 1385 cm^{-1} and deep and wide peak at 1568 cm^{-1} are due to C=C stretches of aromatic rings. Furthermore, the 1223 cm^{-1} peak can be ascribed to the C-O stretching in ethers, alcohols, and/or phenols. The FTIR outcomes clarify that the condition of pyrolysis has a great impact on the adsorption capacity of Iodine in terms of the hydrogen bond capacity created on the biochar materials.

Furthermore, the hydrophobic sites could be originated from the graphitic structure of biochar which is assumed to be interacting with hydrophobic molecules of the biochar. However, the adsorption isotherm results can corroborate this phenomenon. For the tree bark materials, the adsorption kinetic results are shown in **Figure 3c** and **d** and **Table 3** and **Table 3** revealed that the kinetic model fits follow the order $\text{PSO} > \text{Elovich} > \text{PFO} > \text{IPD}$ yet for the Matamba fruit shell, Elovich model fitted the adsorption data better than other kinetic models.

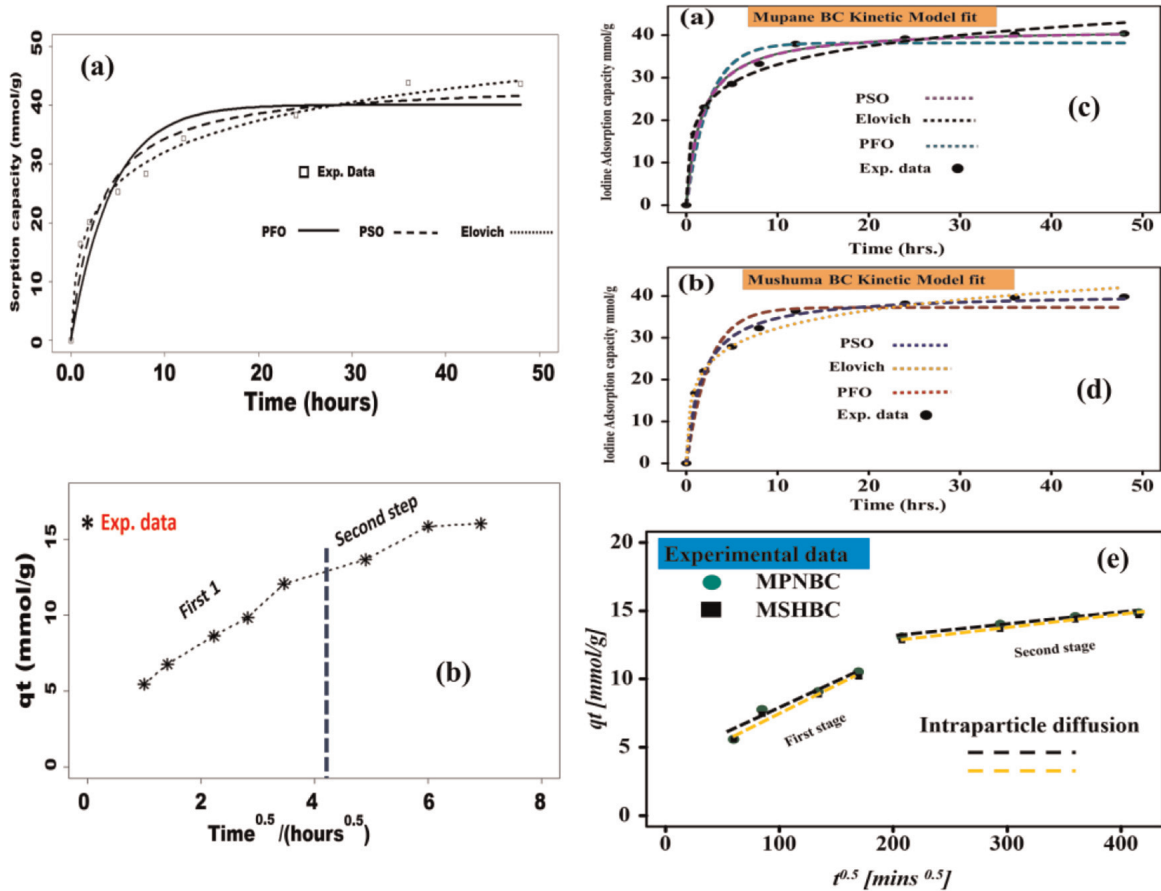


Figure 3. The results from the kinetic adsorption experimental model analysis of biochar materials (a), (c), (d) are PFO, PSO, and Elovich models respectively, and (b), (e) are IPD models correspondingly.

4.2 Langmuir and Freundlich isotherms on Matamba fruit shell

Langmuir and Freundlich isotherm models (Eq. (5)) and (Eq. (6)) were used to examine and investigate the adsorption mechanisms of iodine onto the biochar surface. The Langmuir model described well the removal of iodine with the AICc of 0.527 (lower than 5.377 of the Freundlich model), which exhibited monolayer sorption on the Biochar surface with determinate indistinguishable adsorption sites.

Additionally, Bayesian statistics exhibited a clear difference between the two models from the ggplot2 since Freundlich (**Figure 4d**) shows a wider prediction band than Langmuir (**Figure 4c**). The maximum capacity of adsorption deliberated from the Langmuir model was so vital in biochar surface area estimation. The Matamba fruit shell biochar surface area was estimated to be $267.9 \text{ m}^2 \text{ g}^{-1}$ and $267.6 \text{ m}^2 \text{ g}^{-1}$ from NLS and Bayesian approaches respectively. The biochar surface area was estimated from Iodine adsorption using (Eq. (7)), whereas the Langmuir and Freundlich models reiterate that:

$$q_e = \frac{q_m k_L c_e}{1 + k_L c_e} \quad (1)$$

$$q_e = k_f c_e^{mf} \quad (2)$$

$$\text{SAr} = qt * 10 - 3 * \text{NA} * \omega I \quad (3)$$

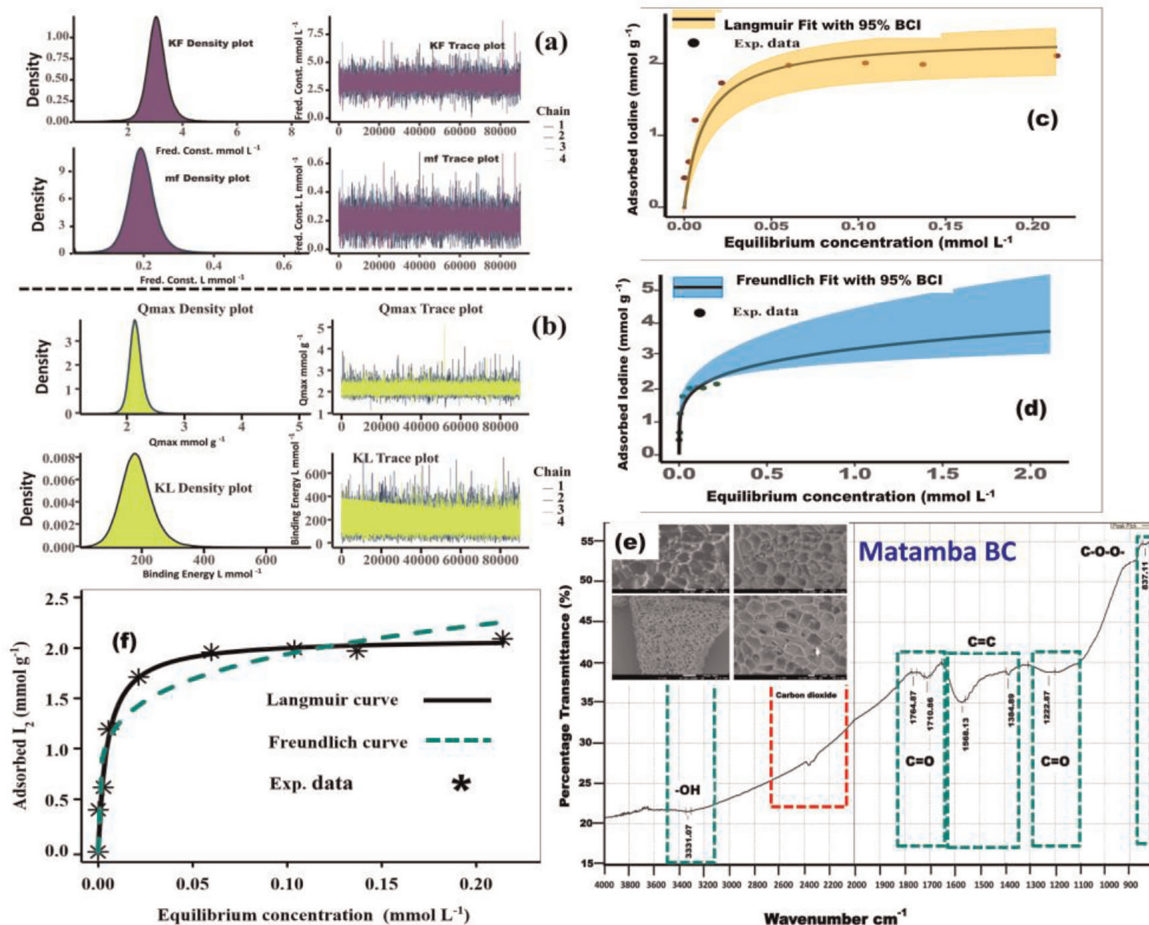


Figure 4. (a) *Freundlich* and (b) *Langmuir* model density curves, (c) 95% Bayesian C.I. analysis of *Langmuir* and (d) *Freundlich* adsorption models, (e) FTIR and FESEM for *Matamba* biochar, (f) *Langmuir* and *Freundlich* adsorption models with conventional analysis method.

Where qm is the maximum adsorption capacity (mmol g^{-1}), k_L is Langmuir constant (L mmol^{-1} , C_e is the equilibrium concentration (mmol L^{-1}), k_f (mmol L mmol^{-1}), and m_f are Freundlich constants. From this q_t is the maximum capacity of adsorption at equilibrium mmol/g , N_A is the Avogadro constant, $N_A = 6.023 \times 10^{23} \text{ mol}^{-1}$, and ω_I is the surface area occupied by one iodine molecule ($0.2096 \times 10^{-18} \text{ m}^2$).

The surface area estimated from both Bayesian and Conventional statistics is insignificant since the q_{max} parameter (Figure 5a–d) only underscores the capacity of the biochar to adsorb the adsorbate yet has less substantial than the K_L as explained by [40]. The high value of the K_L parameter from the MCMC in Figure 5 is directly proportional to the observed surface area because iodine molecules are small enough and strong to be attached to the biochar surface with minimum effects of desorption.

4.3 Statistical analysis using a Bayesian framework

The Bayesian statistics obtains q_{max} of 2.12 mmol g^{-1} and Conventional statistics resulted in the maximum adsorption capacity (q_{max}) of $2.122 \text{ mmol g}^{-1}$. Moreover, the median value was estimated to be 2.12 mmol g^{-1} , whereas the MAP value of 2.11 mmol g^{-1} was obtained and there were no significant differences with the q_{max} . The R_{hat} between 1.05 and 0.9 is acceptable and helps in the rejection of the Markov

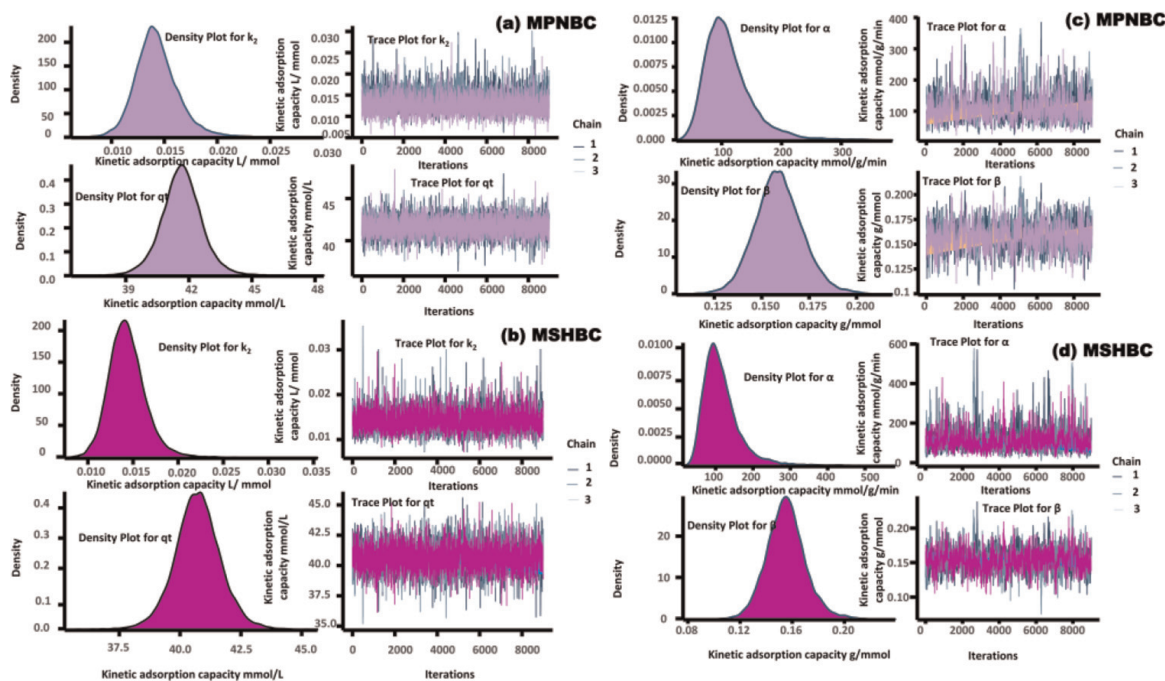


Figure 5. Shows the MCMC density presentation of MPNBC and MSHBC from the Bayesian simulation of PSO and Elovich model's posterior probability distribution mean parameters.

chain Monte Carlo (MCMC) data simulation as it is far away from this range. The Bayesian statistics estimated that the energy binding strength (K_L) to be higher than the NLS, this is shown in **Table 2** where $218.5 \text{ L mmol}^{-1}$ and $206.43 \text{ L mmol}^{-1}$ were observed for the Bayesian and NLS observed respectively.

The K_L results exhibited a stronger evaluation as depicted by the Bayesian method than conventional adsorption, so, Bayesian statistics seem to have a great capacity to estimate isotherm and kinetics parameters with consistency and supporting evidence than the former. The K_L is more significant as estimated by the Bayesian analysis and designated the degree of interface among iodine solution and the biochar surface property. Higher values of the K_L relatively resemble a strong interaction or sorption affinity of the adsorbate concentration onto the adsorbent as large values of K_L reflect the greater force of binding on the biochar material's surface [41, 42].

5. Conclusions

The pyrolysis condition at 600°C revealed the surface characteristics and adsorption mechanisms of the biochar materials to be sufficient in generating adequate biochar for the purpose. These agro-biomass materials used in this study were the first to be investigated for their potential application as low-cost adsorbents in rural areas of Zimbabwe for environmental protection. Easy access to these materials as well as lower production cost makes them fit to solve the water shortages and remove unwanted substances from the environment through adsorption. Elovich and PSO models fitted the data in this study, and this exhibits a heterogeneous surface characteristic of the biochar materials with significant chemisorption mechanisms developed during pyrolysis of the agro-biobased biochar. Bayesian statistical analysis has exhibited slightly higher qt estimations of 40.712 and 41.639 mmol/g when compared to the conventional statistics with 40.01 and 40.29 mmol/g for Mushuma and Mupane

biochar. The Elovich model subsequently described the results very well, henceforth representing a heterogenous surface property with chemisorption phenomena. FESEM-EDX Spectroscopy also revealed that C (81.93 mol% and 86.91 mol %) and O (16.12 mol% and 11.49 mol%) for Mushuma and Mupane respectively. These percentages agreed with the FTIR results where the surface physical properties designated a rich surface with fundamental functional groups and, as a recommendation with the cost for future research, activating these materials could make them enduring adsorbents. The investigation outcomes unveiled the competence and potential of the locally obtainable and produced biochar in removing Iodine solution as affordable materials that can be established for other emerging contaminants and unwanted pollutants from the environment as water reuse and recycling strategy in developing countries and unserved communities and as a climate change mitigatory measure. Matamba, Museum, and Mupane biochar materials are locally available, no costs are required to obtain them, and the benefits of wastewater recycling strategy should be adopted with a proper design fit for rural communities as off-the-grid technology.

Acknowledgements

The authors would like to thank Nagasaki University, Graduate School of Engineering, for the provision of resources, chemicals, and analytical equipment that made this work a success. The authors appreciate the referees, editors, and reviewers for their effort in their correction and suggestions to improve the quality and content of this paper.

Conflict of interest

The authors declare that they have no known competing interests.

Notes/thanks/other declarations

Most acknowledgment is given to the JICA and HONJO Scholarship Foundation for the provision of these Scholarships to be in Japan for the study period.

IntechOpen

Author details

Obey Gotore^{1*}, Tirivashe Phillip Masere², Osamu Nakagoe¹, Vadzanayi Mushayi³,
Ramaraj Rameshprabu⁴, Yuwalee Unpaprom⁴ and Tomoaki Itayama¹

1 Nagasaki University, Nagasaki, Japan


2 Midlands State University, Gweru, Zimbabwe

3 Harare Polytechnic College, Harare, Zimbabwe

4 Maejo University, Chiang Mai, Thailand

*Address all correspondence to: gotoreobey@gmail.com

IntechOpen

© 2022 The Author(s). Licensee IntechOpen. This chapter is distributed under the terms of the Creative Commons Attribution License (<http://creativecommons.org/licenses/by/3.0>), which permits unrestricted use, distribution, and reproduction in any medium, provided the original work is properly cited. 

References

- [1] Abedin M, Collins AE, Habiba U, Shaw R. Climate change, water scarcity, and health adaptation in southwestern coastal Bangladesh. *International Journal of Disaster Risk Science*. 2019;**10**(1): 28-42. DOI: 10.1007/s13753-018-0211-8
- [2] Hanna R, Oliva P. Implications of climate change for children in developing countries. *The Future of Children*. 2016;**26**:115-132. DOI: 10.1353/foc.2016.0006
- [3] Liu X, Tian J, Li Y, Sun N, Mi S, Xie Y, et al. Enhanced dyes adsorption from wastewater via Fe₃O₄ nanoparticles functionalized activated carbon. *Journal of Hazardous Materials*. 2019;**373**: 397-407. DOI: 10.1016/j.jhazmat.2019.03.103
- [4] Bekçi Z, Özveri C, Seki Y, Yurdakoç K. Sorption of malachite green on chitosan bead. *Journal of Hazardous Materials*. 2008;**154**(1-3):254-261. DOI: 10.1016/j.jhazmat.2007.10.021
- [5] Zhou L, Liu Y, Liu S, Yin Y, Zeng G, Tan X, et al. Investigation of the adsorption-reduction mechanisms of hexavalent chromium by ramie biochars of different pyrolytic temperatures. *Bioresource Technology*. 2016;**218**: 351-359. DOI: 10.1016/j.biortech.2016.06.102
- [6] Manea YK, Khan AM, Wani AA, Saleh MA, Qashqoosh MT, Shahadat M, et al. In-grown flower-like Al-Li/Th-LDH@ CNT nanocomposite for enhanced photocatalytic degradation of MG dye and selective adsorption of Cr (VI). *Journal of Environmental Chemical Engineering*. 2022;**10**(1):106848. DOI: 10.1016/j.jece.2021.106848
- [7] Ghatge S, Yang Y, Ko Y, Yoon Y, Ahn JH, Kim JJ, et al. Degradation of sulfonated polyethylene by a bio-photo-Fenton approach using glucose oxidase immobilized on titanium dioxide. *Journal of Hazardous Materials*. 2022; **423**:127067. DOI: 10.1016/j.jhazmat.2021.127067
- [8] Kodavatiganti S, Bhat AP, Gogate PR. Intensified degradation of acid violet 7 dye using ultrasound combined with hydrogen peroxide, Fenton, and persulfate. *Separation and Purification Technology*. 2021;**279**:119673. DOI: 10.1016/j.seppur.2021.119673
- [9] Gotore O, Rameshprabu R, Itayama T. Adsorption performances of corn cob-derived biochar in saturated and semi-saturated vertical-flow constructed wetlands for nutrient removal under erratic oxygen supply. *Environmental Chemistry and Ecotoxicology*. 2022;**4**:155-163. DOI: 10.1016/j.encco.2022.05.001
- [10] Prajapati AK, Mondal MK. Comprehensive kinetic and mass transfer modeling for methylene blue dye adsorption onto CuO nanoparticles loaded on nanoporous activated carbon prepared from waste coconut shell. *Journal of Molecular Liquids*. 2020;**307**: 112949. DOI: 10.1016/j.molliq.2020.112949
- [11] Obey G, Adelaide M, Ramaraj R. Biochar derived from non-customized Matamba fruit shell as an adsorbent for wastewater treatment. *Journal of Bioresources and Bioproducts*. 2022;**7**(2): 109-115. DOI: 10.1016/j.jobab.2021.12.001
- [12] Castiglioni M, Rivoira L, Ingrand I, Meucci L, Binetti R, Fungi M, et al. Biochars intended for water filtration: A comparative study with activated

carbons of their physicochemical properties and removal efficiency towards neutral and anionic organic pollutants. *Chemosphere*. 2022;**288**: 132538. DOI: 10.3390/en14248472

[13] Lesaoana M, Mlaba RP, Mtunzi FM, Klink MJ, Ejidike P, Pakade VE. Influence of inorganic acid modification on Cr (VI) adsorption performance and the physicochemical properties of activated carbon. *South African Journal of Chemical Engineering*. 2019;**28**:8-18. DOI: 10.1016/j.sajce.2019.01.001

[14] Cong L, Feng L, Wei X, Jin J, Wu K. Study on the adsorption characteristics of Congo red by sycamore bark activated carbon. In: ENVIRONMENT. TECHNOLOGIES. RESOURCES. Proceedings of the International Scientific and Practical Conference. Republic of Latvia: The scientific journal of rezeke academy of technologies; Vol. 1. 2017. pp. 64-69. DOI: 10.17770/etr2017vol1.2600

[15] Gautam UK, Panchakarla LS, Dierre B, Fang X, Bando Y, Sekiguchi T, et al. Solvothermal synthesis, cathodoluminescence, and field-emission properties of pure and N-doped ZnO nano bullets. *Advanced Functional Materials*. 2009;**19**(1):131-140. DOI: 10.1002/adfm.200801259

[16] Talha MA, Goswami M, Giri BS, Sharma A, Rai BN, Singh RS. Bioremediation of Congo red dye in immobilized batch and continuous packed bed bioreactor by *Brevibacillus parabrevis* using coconut shell bio-char. *Bioresource Technology*. 2018;**252**:37-43. DOI: 10.1016/j.biortech.2017.12.081

[17] Fu MM, Mo CH, Li H, Zhang YN, Huang WX, Wong MH. Comparison of physicochemical properties of biochars

and hydrochars produced from food wastes. *Journal of Cleaner Production*. 2019;**236**:117637. DOI: 10.1016/j.jclepro.2019.117637

[18] Sriburi T, Wijitkosum S. Biochar amendment experiments in Thailand: Practical examples. In: Bruckman VJ, Klinglmüller M, editors. *Potentials to Mitigate Climate Change Using Biochar*. Cambridge, United Kingdom: Cambridge University Press; 2016

[19] O'Connor D, Peng TY, Zhang JL, Tsang DCW, Alessi DS, Shen ZT, et al. Biochar application for the remediation of heavy metal polluted land: A review of *in situ* field trials. *Science of the Total Environment*. 2018;**619**(620):815-826. DOI: 10.1016/j.scitotenv.2017.11.132

[20] Chandra S, Bhattacharya J. Influence of temperature and duration of pyrolysis on the property heterogeneity of rice straw biochar and optimization of pyrolysis conditions for its application in soils. *Journal of Cleaner Production*. 2019;**215**:1123-1139. DOI: 10.1016/j.jclepro.2019.01.079

[21] Kambo HS, Dutta A. A comparative review of biochar and hydrochar in terms of production, physico-chemical properties and applications. *Renewable and Sustainable Energy Reviews*. 2015; **45**:359-378. DOI: 10.1016/j.rser.2015.01.050

[22] Gotore O, Osamu N, Rameshprabu R, Arthi M, Unpaprom Y, Itayama T. Iodine adsorption isotherms on Matamba fruit shell stemmed biochar for wastewater re-use strategy in rural areas owing to climate change. *Chemosphere*. 2022;**303**:135126. DOI: 10.1016/j.chemosphere.2022.135126

[23] Morgan TJ, Turn SQ, George A. Fast pyrolysis behavior of banagrass as a

- function of temperature and volatiles residence time in a fluidized bed reactor. *PLoS One*. 2015;**10**:e0136511. DOI: 10.1371/journal.pone.0136511
- [24] Ngadze RT, Verkerk R, Nyanga LK, Fogliano V, Linnemann AR. Improvement of traditional processing of local monkey orange (*Strychnos spp.*) fruits to enhance nutrition security in Zimbabwe. *Food Security*. 2017;**9**:1-13. DOI: 10.1007/s12571-017-0679-x
- [25] Mwamba CK. *Monkey Orange: Strychnos cocculoides Crops for the Future*. Vol. 8. Southampton Centre for Underutilised Crops, UK; 2006
- [26] National Research Council. *Lost crops of Africa*. In: *Fruits*. Washington DC: The National Academies Press; 2008
- [27] Mwampamba TH, Owen M, Pigaht M. Opportunities, challenges and way forward for the charcoal briquette industry in sub-Saharan Africa. *Energy for Sustainable Development*. 2013;**17**:158-170. DOI: 10.1016/j.esd.2012.10.006
- [28] Ajayi OC, Mafongoya PL. Indigenous knowledge systems and climate change management in Africa. *Africa Report; Technical Center for Agricultural and Rural Cooperation*; 2017. Available online: https://scholar.google.com/scholar_lookup?hl=en&publication_year=2017&author=P.L.+Mafongoya&author=O.C.+Ajayi&title=Indigenous+Knowledge+Systems+and+Climate+Change+Management+in+Africa
- [29] Gotore O, Mushayi V, Rameshprabu R, Gochayi L, Itayama T. Adsorption studies of iodine removal by low-cost bioinspired *Mushuma* and *Mupane* bark derived adsorbents for urban and rural wastewater reuse. *International Journal of Human Capital in Urban Management*. 2022;**7**(3): 297-308. DOI: 10.22034/IJHCUM.2022.03.01
- [30] Taha SM, Amer ME, Elmarsafy AE, Elkady MY. Adsorption of 15 different pesticides on untreated and phosphoric acid treated biochar and charcoal from water. *Journal of Environmental Chemical Engineering*. 2014;**2**:20-25. DOI: 10.1016/j.jece.2014.09.001
- [31] Hevira L, Ighalo JO, Aziz H, Zein R. *Terminalia catappa* shell as low-cost biosorbent for the removal of methylene blue from aqueous solutions. *Journal of Industrial and Engineering Chemistry*. 2021;**97**:188-199. DOI: 10.1016/j.jiec.2021.01.028
- [32] Zazycki MA, Godinho M, Perondi D, Foletto EL, Collazzo GC, Dotto GL. New biochar from pecan nutshells as an alternative adsorbent for removing reactive red 141 from aqueous solutions. *Journal of Cleaner Production*. 2018;**171**: 57-65. DOI: 10.1016/j.jclepro.2017.10.007
- [33] Dotto GL, Pinto LA. Adsorption of food dyes onto chitosan: Optimization process and kinetic. *Carbohydrate Polymers*. 2011;**84**(1):231-238. DOI: 10.1016/j.carbpol.2010.11.028
- [34] Cheung CW, Porter JF, McKay G. Elovich equation and modified second-order equation for sorption of cadmium ions onto bone char. *Journal of Chemical Technology & Biotechnology*. 2000;**75**(11):963-970. DOI: 10.1002/1097-4660(200011)75:11<963::AID-JCTB302>3.0.CO;2-Z
- [35] Dang BT, Gotore O, Ramaraj R, Unpaprom Y, Whangchai N, Bui XT, et al. Sustainability and application of corncob-derived biochar for removal of fluoroquinolones. *Biomass Conversion and Biorefinery*. 2022;**12**(3):913-923. DOI: 10.1007/s13399-020-01222-x

- [36] Doumer ME, Arízaga GG, da Silva DA, Yamamoto CI, Novotny EH, Santos JM, et al. Slow pyrolysis of different Brazilian waste biomasses as sources of soil conditioners and energy, and for environmental protection. *Journal of Analytical and Applied Pyrolysis*. 2015;**113**:434-443. DOI: 10.1016/j.jaap.2015.03.006
- [37] Al-Wabel MI, Al-Omran A, El-Naggar AH, Nadeem M, Usman AR. Pyrolysis temperature induced changes in characteristics and chemical composition of biochar produced from conocarpus wastes. *Bioresource Technology*. 2013;**131**:374-379. DOI: 10.1016/j.biortech.2012.12.165
- [38] Furia CA, Feldt R, Torkar R. Bayesian data analysis in empirical software engineering research. *IEEE Transactions on Software Engineering*. 2019;**47**(9):1786-1810. DOI: 10.1109/TSE.2019.2935974
- [39] Gelman A, Carlin JB, Stern HS, Rubin DB. *Bayesian Data Analysis* Chapman & Hall. Boca Raton, FL, USA: CRC Texts in Statistical Science; 2004
- [40] MacDermid-Watts K, Pradhan R, Dutta A. Catalytic hydrothermal carbonization treatment of biomass for enhanced activated carbon: A review. *Waste and Biomass Valorization*. 2021; **12**(5):2171-2186. DOI: 10.1007/s12649-020-01134-x
- [41] Bandara T, Xu J, Potter ID, Franks A, Chathurika JB, Tang C. Mechanisms for the removal of Cd (II) and Cu (II) from aqueous solution and mine water by biochars derived from agricultural wastes. *Chemosphere*. 2020;**254**:126745. DOI: 10.1016/j.chemosphere.2020.126745
- [42] Devi P, Saroha AK. Improvement in performance of sludge-based adsorbents by controlling key parameters by activation/modification: A critical review. *Critical Reviews in Environmental Science and Technology*. 2016;**46**(21-22):1704-1743. DOI: 10.1080/10643389.2016.1260902